Journal of Applied Mechanics and Technical Physics, Vol. 45, No. 5, pp. 647–655, 2004

NONLINEAR GROUP INTERACTIONS OF THE TAYLOR–GÖRTLER DISTURBANCES IN SUPERSONIC AXISYMMETRIC JETS

N. M. Terekhova

UDC 532.526

The nonlinear group interaction of the Taylor–Görtler disturbances (streamwise vortices) at the initial section of a supersonic axisymmetric jet is numerically studied within the framework of the weakly nonlinear theory of stability. The experimentally observed spectrum of disturbances is considered. The regular and specific features of the streamwise dynamics of various wave components for a turbulent jet are studied. It is shown that such an interaction in the coupled mode in resonant group triplets allows one to describe the experimentally observed elevated growth of background components of the real spectrum.

Key words: *nonisobaric supersonic jet, streamwise vortices, three-wave resonant interactions.*

Introduction. The possibility of three-wave interactions of disturbances of rotational or centrifugal instability (Taylor–Görtler waves) at the initial section of a nonisobaric jet is theoretically analyzed in the present work. Such wave are often called streamwise vortices. This type of instability in jets has been adequately examined both experimentally [1–6] and theoretically [6–12]. In numerical simulations of characteristics of such disturbances, it was found that the regular features of the streamwise dynamics of most azimuthal components of real amplitude spectra can be explained within the framework of the linear stability theory. A fairly extended justification of applicability of the viscid–inviscid approximations was demonstrated in [12] in analyzing the experimental data of [2]. The experiments of [2] currently seem to be the most reliable ones and can be used to verify theoretical models explaining the streamwise evolution of streamwise vortices.

As is known from experience, the real signal of the excessive total pressure, measured in different azimuthal positions of the mixing layer of the jet, is a superposition of spectral wave components of a wide azimuthal composition. The modes observed include background components of moderate intensity, in particular, for [2], this is the mode of the azimuthal number $n = 4$. For such components, an elevated growth of intensity in the downstream direction was observed, with the growth rate much higher than linear. This elevated growth cannot be explained within the framework of the linear stability theory. It becomes necessary to clarify the nature of physical processes inherent in the downstream evolution of such vortices, which involves corrections in theoretical values of wave growth rates.

The objective of the present work is to study the nonlinear interaction of the most typical azimuthal modes. The interaction is studied within the framework of the weakly nonlinear stability theory for three-wave resonant systems including the most representative azimuthal components of the Taylor–Görtler waves. Such a model is the simplest way of considering the nonlinearity as applied to free-stream disturbances. As was shown in [13–15], three-wave resonances of travelling large-scale waves of the Kelvin–Helmholtz instability class are possible, and they offer a qualitatively correct pattern of spectrum filling and evolution of allocated carrier frequencies.

Institute of Theoretical and Applied Mechanics, Siberian Division, Russian Academy of Sciences, Novosibirsk 630090; terekh@itam.nsc.ru. Translated from Prikladnaya Mekhanika i Tekhnicheskaya Fizika, Vol. 45, No. 5, pp. 41–50, September–October, 2004. Original article submitted November 29, 2002; revision submitted February 9, 2004.

In the present work, we consider triplets composed of 10 (in one variant, 11) azimuthal components with wavenumbers $1 \leqslant n \leqslant 10(11)$ satisfying the phase-synchronism conditions. Since three-wave systems for more than three components are considered, such triplets were conventionally called the group triplets; for each component of the real signal, they include a series of simple triplets; the number and composition of waves will be indicated below. The problem is considered in the plane–parallel approximation of the weakly nonlinear stability theory for a compressible inviscid gas.

Basic Equations and Methods of the Solution. The main postulates of this approximation are described in detail in the theoretical papers mentioned above, and here we will only make a brief introduction into the problem formulation. We consider a compressed layer of the first cell of an axisymmetric immersed underexpanded jet: from the external boundary of the barrel shock wave to the near-jet region in the transverse direction and from the nozzle exit to the Mach disk in the longitudinal direction. The barrel-shock position determines the values of the curvature radius R_0 and centrifugal forces proportional to U^2/R_0.

As curvilinear orthogonal coordinates, we choose the radial [$R = R_0 + r$ ($R_0 \gg r$)] and angular [azimuthal (φ) and longitudinal (γ)] variables. They correspond to the radial, azimuthal, and longitudinal components of velocity v, w, and u. The streamwise coordinate x is introduced as $dx = R_0\, d\gamma$. The length of the computational domain in this direction is expressed via the mixing-layer thickness δ. We consider the range of real dimensionless thicknesses $0.1 < \delta < 0.65$. The dependences $\delta(x)$ are described by the expression

$$\delta = \Lambda x + \delta_0, \tag{1}$$

where δ_0 is the initial thickness at $x = 0$, and the coefficient Λ characterizes the growth rate of the layer thickness $\Lambda = d\delta/dx$. The values of Λ depend on the exhaustion regime and are described in more detail below.

The velocity field, density, and pressure are presented as

$$v = \varepsilon v', \quad w = \varepsilon w', \quad u = U(r) + \varepsilon u', \quad \rho = \rho_0(r) + \varepsilon \rho', \quad p = P + \varepsilon p', \tag{2}$$

where the prime indicates disturbances; the scale factor is $\varepsilon \ll 1$.

The disturbances are considered in the compressed layer consisting of two subdomains. In the inviscid subdomain (from the external boundary of the barrel shock to the line of the maximum total pressure), the longitudinal velocity and density are assumed to be constant and equal to their maximum values. In averaging the equations, $\bar{U}$ and the mean density $\bar{\rho}_0$ in this analog of the potential core are assumed to be characteristic values. In the second subdomain (mixing layer), there occurs a smooth transition to ambient parameters. The dimensionless profiles of the mean velocity are set here in the form

$$U(r) = \exp\left(-0.693\eta^2\right), \qquad \eta = 2(r - r_1)/\delta, \qquad r_1 = 1 - \delta/2.$$

The mean density ρ_0 is related to U by the formula

$$\rho_0 = [1 + (k-1)\mathrm{M}_0^2(1 - U^2)/2]^{-1};$$

the velocity of sound is $a = [\rho_0 \mathrm{M}_0^2]^{-1/2}$. The value of the Mach number M_0 is also determined on the line of the maximum velocity.

As the characteristic linear scale $\bar{r}_m$, we use the value of $\bar{r}$ on the half-velocity line; hence, $U = 0.5$ in the dimensionless form for $r = 1$. The value $r = 1$ coincides with the half-thickness of the mixing layer, where $r_1 < r < 1 + \delta/2$.

We seek the wave solutions changing slowly along the streamwise coordinate x (we write expressions for the pressure component only):

$$p'(r, \varphi, x, t) = A(x)p(r)\exp\tau, \qquad \tau = i(\alpha x - \omega t + n\varphi). \tag{3}$$

Here, A is the amplitude (complex quantity), p is the amplitude eigenfunction of the disturbances, $\alpha = \alpha^r + i\alpha^i$, α^r and n are the longitudinal and azimuthal wavenumbers, and α^i is the growth rate in the streamwise direction (increment for $\alpha^i < 0$); the angular frequency ω is real. The value of n determines the number of vortices or vortex pairs over the jet circumference. Low values of n correspond to large-scale vortices, and high values correspond to small-scale vortices. It is assumed that the amplitudes of disturbances with positive and negative n are identical, which yields the classical representation of the Taylor–Görtler waves $p'(r, \varphi, x, t) = A(x)p(r)\exp i(\alpha x - \omega t)\cos n$. The form of Eq. (3) allows more compact further transformations.

Substituting (2) and (3) into the governing equations that describe the motion of an inviscid compressible gas [13–15], after linearization, we obtain the system

$$\mathrm{e}^{\tau}\Big[iFv+\frac{p_r}{\rho_0}-\frac{2Uu}{R}\Big]=-B_1,\quad \mathrm{e}^{\tau}\Big[iFw+\frac{inp}{\rho_0 r}\Big]=-B_2,\quad \mathrm{e}^{\tau}[iFu+U_r v+\frac{i\alpha p}{\rho_0}\Big]=-B_3,$$
$$\mathrm{e}^{\tau}\Big[iF\mathrm{M}_0^2 p+v_r+\frac{v}{r}+\frac{inw}{r}+i\alpha u\Big]=-B_4,\qquad F=\alpha U-\omega \tag{4}$$

with the boundary conditions $p\to 0$ as $r\to 0$ and $r\to\infty$.

It was found by experimental methods that the Taylor–Görtler disturbances are stationary or quasi-stationary; the values of α^r and ω are close to zero; hence, to avoid singularities in integration of the governing equations as $U\to 0$, the computations were performed for small ω set via the acoustic Strouhal number $\mathrm{Sh}=2\pi\bar{\omega}\bar{r}/\bar{a}$, where $\bar{a}$ is the velocity of sound in the external field. Normally, we used $\mathrm{Sh}=0.005$; in this case, $\alpha^r\approx 0$. In Eq. (4), we take into account only the main centrifugal term in the first equation for v.

The nonlinear coefficients B have the form

$$B_1=v'v'_r+\frac{w'v'_\varphi}{r}+u'v'_x-\frac{w'^2}{r}-\frac{u'^2}{R}-\frac{\rho' p'_r}{\rho_0^2},$$

$$B_2=v'w'_r+\frac{w'w'_\varphi}{r}+u'w'_x+\frac{v'w'}{r}-\frac{\rho' p'_\varphi}{r\rho_0^2},\qquad B_3=v'u'_r+\frac{w'u'_\varphi}{r}+u'u'_x-\frac{\rho' p'_x}{\rho_0^2},$$

$$B_4=\frac{1}{a^2}\Big\{\Big(\frac{\rho'}{\rho_0}-\frac{p'}{P}\Big)(p'_t+Up'_x)+v'p'_r+\frac{w'p'_\varphi}{r}+u'p'_x\Big\}+\rho'\Big(v'_r+\frac{w'_\varphi}{r}+u'_x+\frac{v'}{r}\Big).$$

For linear waves (first-order approximation in terms of ε), the coefficients are $B\equiv 0$, and the amplitude A is indeterminate.

The amplitude functions of the wave components are expressed via the amplitude function of pressure p, and system (4) is solved in terms of p. The reduced equation corresponding to the plane–parallel approximation has the form

$$\mathrm{e}^{\tau}L(p)=N_1,\qquad L(p)\equiv p_{rr}+G_1p_r+G_2p, \tag{5}$$

where $G_1=G_1^0+G_1^R$; $G_2=G_2^0+G_2^R$, $G_1^0=1/r-\rho_{0r}/\rho_0-2F_r/F$, $G_2^0=F^2/a^2-n^2/r^2-\alpha^2$, and the additional terms $G_1^R=2\alpha U/(FR)-2F_rb/(FE)+b_r/E$ and $G_2^R=b((n^2/(rF)^2-1/a^2)+2(F_r-\alpha U(\rho_{0r}/\rho_0+2F_r(1+b/E)/F-b_r/E-1/r))/(FR)$ ($b=2UU_r/R$ and $E=F^2-b$) are determined by the presence of the centrifugal force. The nonlinear terms are

$$N_1\equiv \mathrm{e}^{\tau_1}N=\Big[\frac{dB_1}{dr}+\Big(\frac{1}{r}-2\,\frac{F_r}{F}\Big)B_1+i\,\frac{n}{r}\,B_2+i\alpha B_3-i\,\frac{FB_4}{\rho_0}\Big]\rho_0,$$

where τ_1 is the total phase obtained owing to nonlinear interaction of different components.

The boundary conditions in regions of constant mean parameters are expressed via the modified Bessel functions of the first kind I^n and second kind K^n:

$$p=C_1I^n(z_1),\qquad p_r=C_1I^n_z(z_1),\qquad r\to 0,$$
$$p=C_2K^n(z_2),\qquad p_r=C_2K^n_z(z_2),\qquad r\to\infty, \tag{6}$$
$$z=\lambda r,\qquad \lambda^2=F^2/a^2-\alpha^2.$$

The above-formulated boundary eigenvalue problem allows us to determine the eigenvalue of α^i for given M_0, δ, R_0, and n. The corresponding eigenfunction p obtained by normalization $p_{\max}=1$ has an arbitrary amplitude A.

We write the mutual effect of disturbances satisfying the conditions of phase synchronism as $\tau_j=\tau_1$, where $\tau_1=\tau_l+\tau_k$; the subscripts indicate the corresponding interacting waves. Normally, $j\ne l\ne k$, though there are triplets with $k=l$, they describe self-action effects.

Performing averaging and using the solvability conditions [16], we find the amplitude equations that describe the streamwise evolution of wave amplitudes in group triplets:

$$\frac{dA_j}{dx} = -\alpha_j^i A_j + \sum_{l,k} K_{l,k} A_l A_k,$$

$$\frac{dA_l}{dx} = -\alpha_l^i A_l + \sum_{j,k} K_{j,k}^* A_j A_k^*, \qquad \frac{dA_k}{dx} = -\alpha_k^i A_k + \sum_{j,l} K_{j,l}^* A_j A_l^*. \tag{7}$$

Here,

$$K_{l,k} = \int_0^\infty p_j^+ N_{l,k}\, dr \Big/ \int_0^\infty p_j^+ \frac{\partial L(p_j)}{\partial \alpha_j}\, dr$$

(p^+ is the solution of the equation conjugate with the homogeneous equation [13–15]). It can be derived from (5) as

$$p_{rr}^+ - (G_1 p^+)_r + G_2 p^+ = 0,$$

and the boundary conditions are determined from (6) and the bilinear form $\phi[pp^+] \equiv pp^+/r + p_r p^+ - pp_r^+ = 0$.

The amplitudes A are written in an exponential form $A_j = |A_j|\, \mathrm{e}^{i\psi_j}$, and Eqs. (7) are solved for the absolute values of amplitudes $|A_j|$ and amplitude phases $\psi_j = \operatorname{Arg} A_j$ with initial conditions corresponding to [2].

Let us make some necessary comments. Azimuthal sweep diagrams of the excessive total pressure δP_0 in different longitudinal sections of the first cell (barrel) of the jet were obtained in [2]. These data were processed in [12]. The values of δP_0 cited in [2] were expanded into the Fourier series, and the spectral components of the series were identified with the azimuthal components of the Taylor–Görtler disturbances. This allowed us to obtain the absolute values of the excessive total pressure (intensity I), the phase characteristics ψ of all modes of the signal for different x, and the spatial growth rates $-\alpha^i = (x_1 - x_0)^{-1} \ln[I(x_1)/I(x_0)]$.

The initial values of amplitudes $|A_j(x_0)|$ are found from the intensities of total pressures in the initial cross section x_0 as $I_j(x_0) = |A_j(x_0)|\, |\delta P_0(x_0)| \exp(-\alpha^i x_0)$, where $|\delta P_0|$ is the maximum calculated absolute value of the total pressure disturbance along the transverse coordinate. It is constructed on the basis of the known gas-dynamic relation, which, with accuracy to quadratic terms, yields [7–11, 15] $\delta P_0/P_0 = [p/P + k\mathrm{M}^2((1-k)p/(kP) + 2u/U)]/(2 + (k-1)\mathrm{M}^2)$, where M is the local Mach number and $k = C_P/C_V$. In (7), the initial conditions $\psi_j(x_0)$ for different values of n were also consistent with the data of [2].

We denote the streamwise growth rate of the corresponding azimuthal mode as β_j; this is a nonlinear increment of the order of $O(\varepsilon^2)$:

$$\beta_j \equiv \operatorname{Real} \frac{d \ln \delta P_{0j}}{dx} = \operatorname{Real} \Big(i\alpha_j + \frac{d \ln |A_j|}{dx} \Big).$$

The first term in this expression is the linear growth rate; the second term determines the contribution of nonlinear interaction in the resonant mode.

Results and Discussion. As was mentioned above, the basis for determining the components of nonlinear consideration was the experimental data of [2] for an underexpanded jet with the jet pressure ratio of ≈4.5, $\mathrm{M}_0 = 1.5$, $k = 1.4$, and $R_0 \approx 10$–15. It was shown in [12] that the real signal in the first cell of the jet is a superposition of components with $1 \leqslant n \leqslant 30$ with different intensities I. Some of them (those with high azimuthal wavenumbers n) are background components; an essential contribution to δP_0 is made by modes with $n < 14$.

Figure 1 shows the intensities (I) in an arbitrary scale and the phases (ψ) in radians in the initial and final measurement sections [2]. Wave components with intensities lower than five percent of the mean total pressure $I_n/I_0 < 0.05$ are assumed to be background components; they are indicated by the dashed curve in the figure. Note, the growth rate for the background component with $n = 4$ is rather significant. Nonlinearity is expected to be important for those modes for which changes in phase values were noticed.

In the present work, we consider the range $1 \leqslant n \leqslant 10$ for moderate values of R_0 and the range $1 \leqslant n \leqslant 11$ for high R_0. For these modes, the group interaction in resonant triads was numerically simulated within the framework of the nonlinear model of the second order in terms of disturbance amplitudes. High values of the curvature radius R_0 were considered to find the effect of this governing parameter of the problem.

Since the values of ω and α^r for the Taylor–Görtler waves are not very high, the phase-synchronism conditions are determined only by the values of azimuthal wavenumbers n: $n_j = n_l + n_k$. By a simple search, we can easily

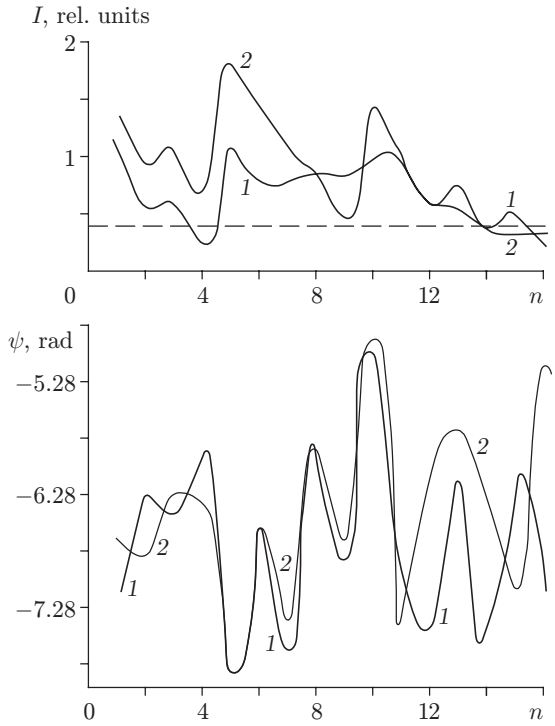

Fig. 1

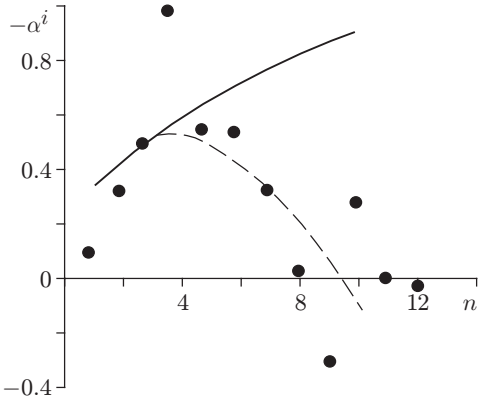

Fig. 2

Fig. 1. Amplitude and phase compositions of the real signal [2] in the initial ($x_0/D = 1.7$) and final ($x/D = 2.5$) sections (curves 1 and 2, respectively).

Fig. 2. Linear growth rates of the Taylor–Görtler waves for $\delta = 0.4$ and $R_0 = 10$: curve 1 refers to inviscid approximation and curve 2 refers to viscid approximation with Prandtl-based turbulent viscosity; $\mathrm{Re}_t = 300$; the points show the experiments growth rates [2].

find that the total number of simple triplets is 30 for the nonlinear group interaction of 11 modes. The group triplet consists of 5 simple triplets for the highest mode $n = 11$ and of 10 simple triplets for the lowest mode $n = 1$. Triplets relating the like components take into account the effect of self-action and possible redistribution of energy of this component and the mode with a doubled wavenumber in this process. If the number of interacting modes is 10, the group triplet consists of 25 simple triplets.

The solid curve in Fig. 2 shows the growth rates $-\alpha^i$ for the azimuthal components considered and for the mixing-layer thickness $\delta = 0.4$, which were obtained within the framework of the inviscid approximation of the linear stability theory. Note, for modes with moderate n, the values of the linear growth rates depend rather weakly on δ, and the pattern shown rather adequately reflects their relation in the mixing layer of the first cell of the jet, obtained in this kind of simulation.

As was found in experiments, however, for turbulent jets (and these were the regimes considered), the real growth rates start to deviate from these inviscid dependences with increasing azimuthal wavenumber n, and their values are significantly lower than the calculated ones. Figure 2 shows the growth rates obtained in [12] on the basis of the experiments of [2]; these data were used for comparisons with the numerical simulation results.

It was shown [10] that these deviations can be attributed to the effect of viscosity. In the experiments considered, the exhaustion occurs in the regime of developed turbulence; hence, turbulent viscosity should be taken into account for an adequate theoretical description of growth rates in the entire range of existence of growing oscillations. Reliable models of turbulence for gradientless free flows of the jet and wake types have not been constructed yet, and we have to seek the regular features at the qualitative level. We use Prandtl's simple algebraic model of turbulence [17]. In this model, the turbulent scale $\bar{\nu}_t = \bar{l}^2 \left|\partial \bar{U}/\partial \bar{r}\right|$ is expressed via the mixing length $\bar{l}$, which, for a compressible free flow, is written as $\bar{l} = c\delta \bar{r}_m$; in the coefficient c, compressibility is taken into account

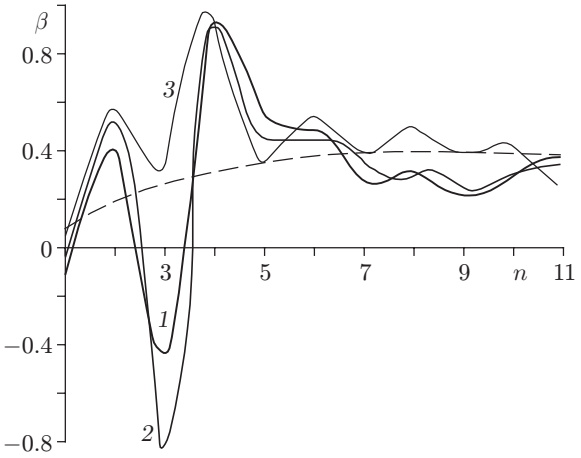

Fig. 3

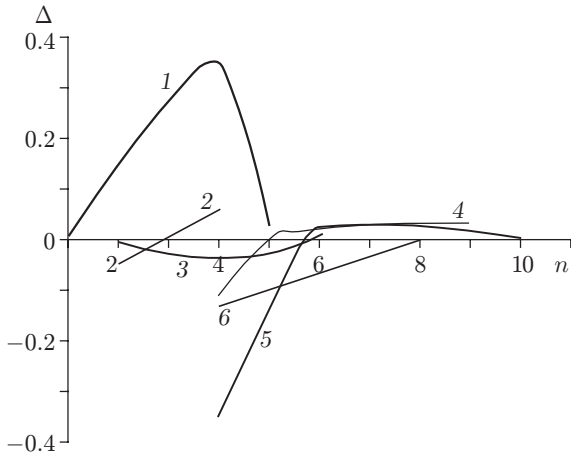

Fig. 4

Fig. 3. Effect of the jet-exhaustion regime on nonlinear growth rates: curves 1 and 2 refer to turbulent jet for $\Lambda_1 = 0.2281$ and $\Lambda_2 = 0.158$, respectively; curves 3 refers to laminar jet for $\Lambda_3 = 0.083$; the dashed curve shows the linear growth rates predicted by the inviscid model.

Fig. 4. Difference in nonlinear and linear growth rates in simple triplets $n_j = n_k + n_l$ including the mode $n_j = 4$: triplets with modes $4 = 5 - 1$ (curve 1), $4 = 2 + 2$ (curve 2), $4 = 6 - 2$ (curve 3), $4 = 9 - 5$ (curve 4), $4 = 10 - 6$ (curve 5), and $4 = 8 - 4$ (curve 6).

by the empirical relation $c = 0.09 - \sqrt{\mathrm{M} - 1.2}/42$ $(1.2 \leqslant \mathrm{M} \leqslant 3.6)$. The values of the Reynolds number with turbulent viscosity are determined by the relation $\mathrm{Re}_t = \bar{U}\bar{l}/\bar{\nu}_t$.

For the reconstructed exhaustion parameters, it was found that the values of Re_t are within the range $300 \leqslant \mathrm{Re}_t \leqslant 450$. The dashed curve in Fig. 2 shows the linear growth rates with allowance for turbulent viscosity for $\mathrm{Re}_t = 300$. It becomes clear that there exists a range of moderate values of azimuthal components whose linear growth rates are well described by the inviscid approximation. Outside this region, turbulent viscosity should be taken into account, which allows one to obtain a qualitatively correct description of specific features observed in experiments.

In the present paper, we consider three exhaustion regimes [11] determining different values of the growth-rate coefficient Λ for $\mathrm{M}_0 = 1.5$:

1) for a turbulent jet with a large pressure ratio ($\Lambda_1 = 0.2281$);

2) for a turbulent jet with a small pressure ratio ($\Lambda_2 = 0.158$);

3) for the laminar regime ($\Lambda_3 = 0.083$).

Figure 3 shows the values of β for the group triplet consisting of 11 modes for the curvature radius $R_0 = 30$ and different Λ (curves 1–3), as compared to the linear growth rate $-\alpha^i$. The effect of the expansion ratio on the growth rates of most modes is not very substantial. The only specific mode is the mode with $n = 3$ whose growth rate strongly depends on the exhaustion regime and on the value of Λ. The reason for this strong effect has not been found yet.

All subsequent computations were performed for the second variant, which most probably occurs in experiments. Figure 4 illustrates the necessity of considering exactly the group triplet including the greatest possible number of azimuthal components. For $R_0 = 10$, Fig. 4 shows the difference between nonlinear and linear growth rates $\Delta = \beta - \alpha^i$, which were obtained by simulating simple triplets including the mode with $n = 4$. It become clear from Fig. 4 that the energy redistribution in these triplets is absolutely arbitrary and unpredictable; certain modes are characterized by an elevated growth rate, retain a linear growth rate, and become decaying in different triplets. Only triplets simulating the processes of self-action have single-type dynamics: energy transfer to modes with doubled n is always accompanied by a decrease in intensity of the basic mode.

Figure 5 is a key figure: it shows the growth rates β for group triplets including different numbers of azimuthal components on the background of linear growth rates (dashed curves). The main variant — 10 interacting modes

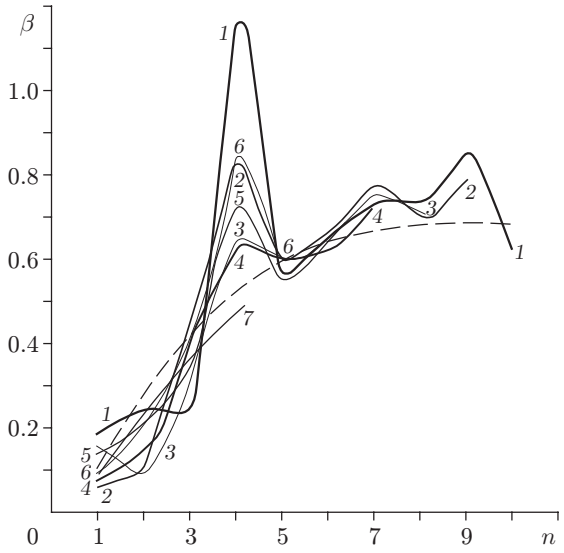

Fig. 5. Nonlinear growth rates (for $R_0 = 10$ and $\delta = 0.5$) of the group triplet composed of 10 (curve 1), 9 (curve 2), 8 (curve 3), 7 (curve 4), 6 (curve 5), 5 (curve 6), and 4 modes (curve 7); the dashed curve shows the linear growth rate.

(25 single triplets) — is shown by curve 1. It is clear that nonlinear interaction is responsible for the increased growth of the background mode $n = 4$; an increase in growth rate is also observed for the modes with $n = 1$, 7, and 9; the modes with $n = 5$, 6, and 8 retain their linear growth rate; the growth rates for the modes with $n = 2$, 3, and 10 becomes slower. Nevertheless, all changes in these components are incommensurable with the growth rate of the mode with $n = 4$, which leads us to a conclusion that exactly nonlinear interaction is the reason for the significant growth rate of this component, as compared to the linear case.

An attempt was made to find out which modes are necessary for the sought features to be realized. This study involved consecutive elimination of higher modes from consideration. Curve 2 shows the group triplet of 9 modes ($1 \leqslant n \leqslant 9$; 20 simple triplets). The growth rate of the mode with $n = 4$ decreases, and the growth rate of the mode with $n = 3$ increases. It becomes clear that the influence of the mode with $n = 10$ on the streamwise dynamics is fairly significant. The growth rates of the lowest modes decrease, and the growth rates of the rest modes change insignificantly. No qualitative changes were found for group triplets composed of 8, 7, and 6 modes. Let us consider the triplet composed of 5 modes in more detail (6 simple triplets; curve 6 in Fig. 5); its action leads to a significant growth of the mode with $n = 4$. It follows from here that the mode with $n = 5$ is also very important for nonlinear evolution of the background mode.

Nonlinear interaction in triplets composed of components with moderate azimuthal numbers n yields lower growth rates as compared to the linear values. Hence, we can conclude that, in modeling the real dynamics of the Taylor–Görtler waves, one should take into account the greatest possible number of components of the experimentally observed value of the excessive total pressure.

In the variants considered above, the linear growth rates of higher modes were presented by their values obtained in the inviscid approximation, which is not the case (as is shown in Fig. 2). Therefore, we performed computations with allowance for the real decrease in linear growth rates of higher modes due to turbulent viscosity.

Figure 6 illustrates the influence of this fact by the example of a group triplet composed of 10 modes for $R_0 = 30$. We consider group triplets with linear growth rates in the inviscid approximation (curves 1) and with allowance for the decrease in growth rates of higher modes (curves 2); we used $\alpha^i_{n=6} = \alpha^i_{n=5}$, $\alpha^i_{n=7} = \alpha^i_{n=4}$, $\alpha^i_{n=8} = \alpha^i_{n=3}$, $\alpha^i_{n=9} = \alpha^i_{n=2}$, and $\alpha^i_{n=10} = \alpha^i_{n=1}$. Because of the decrease in linear growth rates of higher modes, their nonlinear growth rates also become different, which has practically no effect on the dynamics of modes with moderate and low values of azimuthal wavenumbers; a substantial increase in the background mode with $n = 4$ is not observed either.

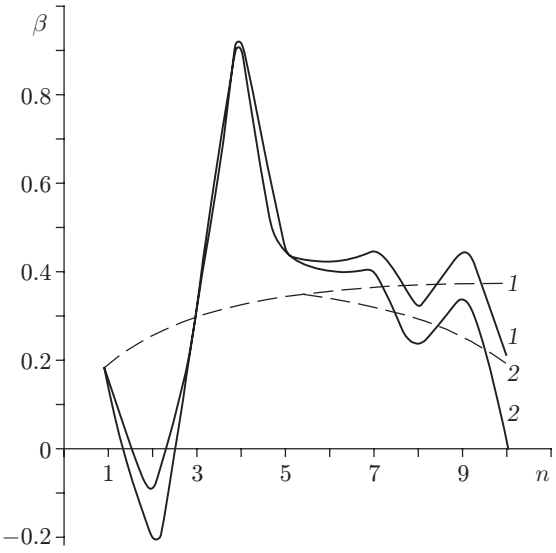

Fig. 6. Modeling of the influence of turbulent viscosity, demonstrating the decrease in linear growth rates of higher modes with $n > 5$. The group triplet is composed of 10 modes for $R_0 = 30$: curve 1 shows the growth rates in the inviscid approximation, curve 2 shows the growth rates with allowance for the decrease, and the dashed curves show the linear growth rates.

Our simulation showed that nonlinear interaction in the jet is possible, but one has to consider the greatest possible number of components to correctly understand this interaction because of the wide range of excited steady components of the real signal. As was shown by numerical calculations, the nonlinearity within the framework of the coupled model in resonant triads affects primarily the dynamics of moderate-intensity modes and leads to elevated growth of these background components.

Unfortunately, universal dependences could not be established here, because the amplitude-spectral composition of the Taylor–Görtler disturbances in jets is determined by the initial background, by the state of the flow on the inner surface of the nozzle, and by the degree of roughness of nozzle edges. This is a specific feature of the nozzle, which induces steady components of different azimuthal compositions and with different phase shifts between one another.

This work was supported by the Council on Grants of the President of the Russian Federation (Grant No. NSh 964.2003.1).

REFERENCES

1. S. A. Novopashin and A. L. Perepelkin, "Self-organization of flow in a supersonic preturbulent jet," Preprint No. 175-88, Inst. of Thermophysics, Sib. Div., Acad. of Sci. of the USSR, Novosibirsk (1988).
2. A. Krothopalli, G. Buzuna, and L. Lourenco, "Streamwise vortices in an underexpanded axisymmetric jet," *Phys. Fluids A*, **3**, No. 8, 1848–1851 (1991).
3. F. P. Welsh and T. M. Cain, "Electron beam visualization of low density nitrogen plumes," in: *Proc. of the 7th Symp. of the Flow Visualization, Seattle* (September 11–15, 1995), Begell House, Inc., New York–Wallingford (1995), pp. 192–197.
4. V. I. Zapryagaev, S. G. Mironov, and A. V. Solotchin, "Spectral composition of wavenumbers of longitudinal vortices and characteristics of the flow structure in a supersonic jet," *J. Appl. Mech. Tech. Phys.*, **34**, No. 5, 634–639 (1993).
5. V. I. Zapryagaev, "The complex investigation method of 3-D disturbances at a curved shear layer of the nonisobaric supersonic jet," in: *Proc. of the 9th Int. Conf. of the Methods of Aerophysical Research*, Part 3, Novosibirsk (1998), pp. 295–300.

6. N. A. Zheltukhin, V. I. Zapryagaev, A. V. Solotchin, and N. M. Terekhova, "Spectral composition and structure of stationary Taylor–Görtler vortices in a supersonic jet," *Dokl. Akad. Nauk SSSR*, **325**, No. 6, 1133–1137 (1992).
7. N. A. Zheltukhin and N. M. Terekhova, "Disturbances of high modes in a supersonic jet," *J. Appl. Mech. Tech. Phys.*, **31**, No. 2, 232–238 (1990).
8. N. A. Zheltukhin and N. M. Terekhova, "Taylor–Görtler instability in a supersonic jet," *J. Appl. Mech. Tech. Phys.*, **34**, No. 5, 640–646 (1993).
9. N. M. Terekhova, "Streamwise vortices in axisymmetric jets," *J. Appl. Mech. Tech. Phys.*, **37**, No. 3, 339–349 (1996).
10. N. M. Terekhova, "Viscous Taylor–Görtler instability in a supersonic axisymmetric jet," *Teplofiz. Aéromekh.*, **6**, No. 3, 307–318 (1999).
11. N. M. Terekhova, "Effect of flow nonparallelism on instability of the Taylor–Görtler waves in supersonic axisymmetric jets," *J. Appl. Mech. Tech. Phys.*, **41**, No. 4, 604–611 (2000).
12. N. M. Terekhova, "Evolution of streamwise vortices in a supersonic axisymmetric jet," *Teplofiz. Aéromekh.*, **8**, No. 3, 423–426 (2001).
13. N. A. Zheltukhin and N. M. Terekhova, "Resonant growth of perturbations in a supersonic jet," *J. Appl. Mech. Tech. Phys.*, **34**, No. 2, 227–232 (1993).
14. N. A. Zheltukhin and N. M. Terekhova, "Three-wave resonant interactions of unstable disturbances in a supersonic jet," *Dokl. Ross. Akad. Nauk*, **334**, No. 2, 168–171 (1994).
15. V. N. Glaznev, V. I. Zapryagaev, V. N. Uskov, et al., *Jets and Unsteady Flows in Gas Dynamics* [in Russian], Izd. Sib. Otd. Ross. Akad. Nauk, Novosibirsk (2000).
16. M. B. Zel'man, "Nonlinear development of disturbances in plane–parallel flows," *Izv. Akad. Nauk SSSR, Ser. Tekh. Nauk*, No. 3, 16–21 (1974).
17. G. N. Abramovich (ed.), *Theory of Turbulent Jets* [in Russian], Nauka, Moscow (1984).